PROTEINS: Structure, Function, and Bioinformatics 56:354–366 (2004)

Predictive Reconstruction of the Mitochondrial Iron–Sulfur Cluster Assembly Metabolism: I. The Role of the Protein Pair Ferredoxin–Ferredoxin Reductase (Yah1–Arh1)

Rui Alves,[1,2]* Enrique Herrero,[1] and Albert Sorribas[1]
[1]*Departament de Ciencies Mediques Basiques, Universidad de Lleida, Lleida, Spain*
[2]*Biomedical Engineering Department, University of California at Davis, Davis, California*

ABSTRACT **Adrenodoxin reductase homologue (Arh1) and yeast adrenodoxin homologue (Yah1) are essential *Saccharomyces cerevisiae* mitochondrial proteins involved in heme A biosynthesis and in iron–sulfur cluster (FeSC) assembly. Although the role of Arh1 and Yah1 in heme A biosynthesis is fairly well established, their systemic role on FeSC synthesis is not well understood. Also, while it is thought that the reductase Arh1 provides electrons for the ferredoxin Yah1, two hybrid experiments do not show interaction between the two proteins. In the first part of this article, we use structural bioinformatics methods to evaluate the possibility of interaction between Arh1 and Yah1. Using protein model building and docking algorithms, we predict a complex between Arh1 and Yah1 that is similar to that of their bovine homologues (adrenodoxin reductase–adrenodoxin reductase), suggesting that Arh1 can indeed reduce Yah1. The predicted complex allows us to suggest point mutations to either molecule that could hinder Arh1–Yah1 interaction and test the role of Arh1 as the reductase for Yah1. In the second part of this article, we investigate the physiological role of Arh1–Yah1 on FeSC assembly by deriving alternative mathematical models of the process, based on published information. Comparing the dynamical behavior of each model with that observed in reported experiments emphasizes the importance of Arh1–Yah1 providing electrons for in situ FeSC repair. Only when this mode of action of either of the two proteins in FeSC synthesis is considered can previously reported results be reproduced. Proteins 2004;56:354–366.**

Key words: kinetic modeling; metabolic reconstruction; systemic biology; structural modeling

INTRODUCTION

Iron–sulfur clusters (FeSC) are widespread cofactors in proteins, working both as catalytic and electron transport mediators and as sensors for the oxidation state of the cellular environment.[1–5] Genetic and biochemical evidence shows that a set of proteins is involved in the proper functioning of FeSC-dependent cellular activity.[2] In *Saccharomyces cerevisiae*, these proteins include GRX5,[6] SSQ1,[7–10] JAC1[7–11] ATM1,[12,13] NFU1,[9,11,14] YAH1,[15] ARH1,[16] ISU1-2,[9,11,17] ISA1-2,[18–20] NFS1,[13,21] YFH1,[22,23] and ERV1.[24] Deficiencies in one or more of these proteins cause impaired FeSC-dependent enzyme activity and mitochondrial iron accumulation, and are connected with Friedriech's ataxia.[25] The systemic role of many of these proteins is not well understood. The goal of this series of articles is to combine the use of different theoretical methods and bioinformatics tools to determine the most likely systemic roles for different FeSC biosynthesis proteins. In this first article of the series, we start by investigating the roles of the ferredoxin–ferredoxin reductase pair, Arh1 and Yah1, respectively.

Adrenodoxin reductase homologue (Arh1) is a mitochondrial essential reductase enzyme in the yeast *S. cerevisiae*.[26] Arh1 is homologous to the mammalian adrenodoxin reductase. Mutations in the latter are complemented by Arh1, although they are involved in different cellular processes.[27,28] Repression of Arh1 expression leads to 10-fold mitochondrial iron accumulation and a 6-fold decrease in FeSC-dependent enzyme activity.[16] Additionally, heme A synthesis is disrupted.[16]

Yeast adrenodoxin homologue (Yah1) is a mitochondrial 2Fe-2S yeast ferredoxin that is homologous to the mammalian adrenodoxin.[29] Contrary to the complementation observed between Arh1 and mammalian adrenodoxin reductase, Yah1 mutants cannot be complemented by the mammalian adrenodoxin.[29] Two hybrid assays have failed to recover a direct interaction between Arh1 and Yah1.[29] The failure may be due to the differences between the nuclear environment of the two-hybrid assay and the mitochondrial environment where the relevant interactions should take place.[30] This negative result is at odds

The Supplementary Materials Referred to in this article can be found at http://www.interscience.wiley.com/jpages/0887-3585/suppmat/index.html

Grant sponsor: Spanish Ministerio de Educacion, Cultura y Deporte; Grant number: SB2000-031 (to R. Alves). Grant sponsor: Portuguese Fundaçao para a Ciencia e Tecnologia (FCT); Grant number: BPD 11533/2002.

*Correspondence to: Rui Alves, Departament de Ciencies Mediques Basiques, Universidad de Lleida, Avenue Rovira Roure 44, 25198 Lleida, Spain. E-mail: ralves@cmb.udl.es

Received 14 September 2003; Accepted 31 December 2003

Published online 7 May 2004 in Wiley InterScience (www.interscience.wiley.com). DOI: 10.1002/prot.20110

with different lines of evidence that support a role for Arh1 as the reductase for Yah1:

1. Repressing the expression of either of the genes—*arh1* or *yah1*—produces the same effects on mitochondrial iron levels, FeSC-dependent enzyme activity, and heme A biosynthesis.[15,29,31]
2. Heme A and FeSC biosynthesis takes place at the mitochondrial matrix, co-localizing with Arh1 and Yah1.[14,32,33]
3. A ferredoxin reductase–ferredoxin pair is thought to be involved in FeSC synthesis in bacteria.[34] This suggests a similar role for the yeast homologues.

The role of Arh1 as the reductase for Yah1 is further supported by their systemic effect in heme A biosynthesis, which is fairly well understood.[31,32,35] Heme A is a fundamental cofactor for cytochrome peroxidase. Near the end of the heme A biosynthetic pathway, coproporphyrinogen III is imported into the mitochondrial matrix and transformed into heme O. Arh1 and Yah1 provide electrons for the final transformation of heme O into heme A.[32] After this transformation, ferrochelatase inserts iron into the protoheme, and the full heme is inserted into the cytochrome peroxidase.

The systemic role of Arh1 or Yah1 on FeSC synthesis is not well understood, although the deletion of either of the genes causes a similar phenotype. FeSC assembly is a process that requires electrons at several different stages. First, iron needs to be reduced to be imported to the mitochondrial matrix.[36] Arh1 and Yah1 could provide electrons to ensure this reduction. However, it has been shown that Yah1 is not involved in mitochondrial iron uptake.[24,36] Second, FeSC clusters are assembled onto scaffold proteins, with the assistance of the cysteine desulfurase Nfs1. Electrons are needed at this stage for the reduction of disulfide bridges and probably also to change the affinity of iron toward the scaffold, thus facilitating the coordination between sulfur and iron in the cluster.[14,37,38] Third, it has been suggested that the redox state of the FeSC transiently assembled in the scaffold proteins determines the affinity of the FeSC to the scaffold and thus the rate of FeSC donation to apo-proteins. Arh1 and Yah1 could provide electrons to regulate this process.[39] Finally, and after transfer of the FeSC to the apo-proteins, the clusters can be damaged. It has been shown that the cysteine desulfurase can repair some of these damaged clusters in situ, instead of reassembling a cluster from the beginning.[40] Arh1 and Yah1 could provide electrons for this process.[15]

In this work we address two questions regarding the Arh1 andYah1 proteins. First, we use structural bioinformatics techniques to investigate whether a protein complex formed by Yah1 and Arh1 could sustain a sufficiently large electron transfer flow to support their as of yet unproven pairing. Our results suggest that this can be the case, and we propose specific experiments to validate our predictions. Second, we address the question of what the direct role of Arh1 and Yah1 is in FeSC assembly by constructing and analyzing mathematical models of alternative networks of Arh1 or Yah1 action on mitochondrial FeSC metabolism. Only when Arh1 or Yah1 donates electrons for the in situ repair of FeSC by Nfs1 can we reproduce previously published experiments. This does not preclude electron donation to other parts of FeSC biosynthesis metabolism but emphasizes the importance of FeSC repair in the dynamics of the system.

METHODS

Structural Homology Modeling and Protein Properties Calculations

If a target protein with undetermined structure has sufficient sequence homology to another protein of known structure, the latter protein can be used as a template to thread the target sequence in three-dimensional (3D) space (see review[41,42]). We use this well-established technique, known as homology modeling, to predict the structures of Arh1 and Yah1. Target and template sequences are aligned using each of the following programs: 3DJIGSAW,[43] SWISSMODEL,[44,45] BONSAI (http://calliope.gs.washington.edu/software/), CLUSTAL,[46] ITERALIGN,[47] and 3D-PSSM.[43] A consensus alignment is then derived (Supplementary Fig. 1). The template files for Arh1 and Yah1 were references 1LQT.pdb and 1E6E.pdb, respectively, from the Protein Data Bank (PDB).[48] These structures were selected because their sequences had the smallest E-values of all candidates with known structures upon alignment to the target proteins. The alignments were submitted to the SWISS-MODEL and 3D-JIGSAW servers for initial structure prediction, and the resulting models were optimized by using DEEPVIEW[44,45] to reconstruct loops and rearrange clashing residues. A full-energy minimization of the models was performed using the GROMACS97 force field.[49] The program ProtParam (http://us.expasy.org/tools/protparam.html) was used to predict in vivo half-life of proteins in yeast cells.

Protein Docking

Given the atomic coordinates of two proteins, docking methods search for the bound complex between them in which the surfaces of the two proteins fit best (see reviews[50,51]). Protein docking experiments were done using GRAMM.[52–54] This method is appropriate for the docking of low-resolution model structures, because it scans the entire protein surfaces against each other, averaging structural details and predicting general features of the ligand–receptor complex.[50,52–54] We used HARLEM[55,56] to predict maximal rates of electron transfer between the proteins of the docked complexes.

Evaluation of the Effect of Arh1 and Yah1 Activity on Mitochondrial FeSC Metabolism

A simplified network describing possible alternative roles for Arh1 and Yah1 in FeSC assembly and transfer is shown in Figure 1. Accessory reactions and rate expressions are presented in Table I. Experimental quantitative data measuring the effect that regulating the gene expression of Arh1 or Yah1 has on FeSC metabolism is available

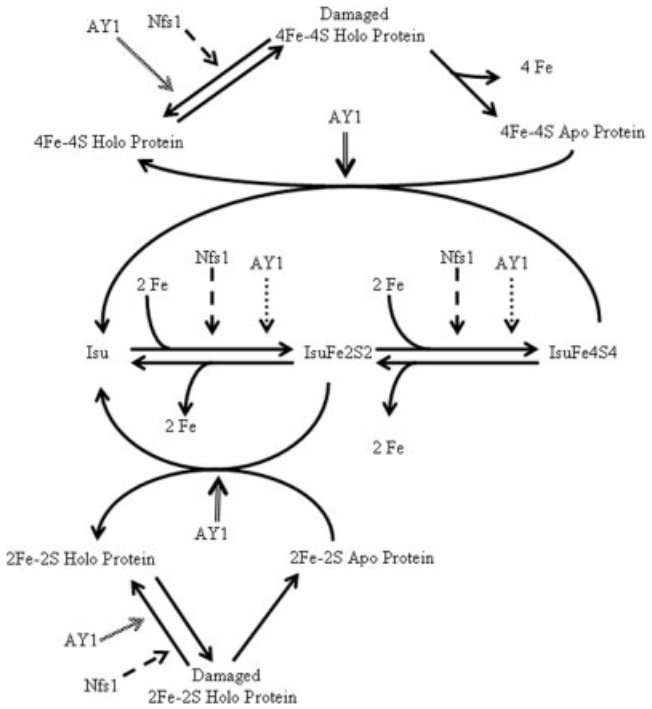

Fig. 1. Alternative roles of Arh1 and Yah1 in the initial FeSC assembly and transfer. Flux of material between different metabolite pools is indicated by full arrows joining the source pool to the sink pool. The catalytic role of a protein in a reaction is represented by broken, dotted, hollow, or lighter shaded arrows, joining the catalytic protein to a full arrow. Isu, pool of free scaffold proteins, where initial assembly of FeSC takes place. IsuFe2S2, pool of scaffold proteins with an assembled 2Fe-2S cluster. IsuFe4S4, pool of scaffold proteins with an assembled 4Fe-4S cluster. 2Fe-2S Apo Protein, 2Fe-2S–dependent apo-protein. 2Fe-2S Holo Protein, fully functional 2Fe-2S–dependent protein. Damaged 2Fe-2S Apo Protein, 2Fe-2S–dependent protein, with a damaged FeSC. 4Fe-4S Apo Protein, 4Fe-4S–dependent apo-protein. 4Fe-4S Holo Protein, fully functional 4Fe-4S–dependent protein. Damaged 4Fe-4S Apo Protein, 4Fe-4S–dependent protein, with a damaged FeSC. Nfs1, cysteine desulfurase, which is the enzyme responsible for FeSC assembly and repair. AY1, Arh1 or Yah1. Clusters initially assemble at the Isu scaffolds. They are transferred from the scaffold to FeSC-dependent apo-proteins. Scaffold and protein FeSC have a natural turnover, and can be damaged and/or lost. Under some conditions, the damaged FeSC can be repaired in situ. Alternative roles that have been proposed for Arh1 and Yah1 in the FeSC assembly metabolism are (1) electron providers for initial FeSC assembly in the scaffold proteins (dotted arrows), (2) electron providers to facilitate FeSC transfer from the scaffold proteins to the FeSC dependent apo-proteins (hollow arrows), and (3) electron providers for in situ repair of damaged FeSC clusters (lighter shaded arrows). For additional reactions and details on rate expressions see the main text of article and Table I.

in the literature.[15,16] These experiments knock out the genes for Arh1 or Yah1, replacing them with the same genes in a plasmid with controllable gene expression. To study the effect of Arh1 or Yah1, the activity of FeSC-dependent enzymes, the mitochondrial iron levels and heme A biosynthesis are monitored at different levels of Arh1 or Yah1 gene expression. To reproduce these experiments in our models, we scan Arh1 or Yah1 activity levels for three orders of magnitude above and below a normalized reference point. We then compute the steady-state relative amounts of FeSC-dependent proteins containing FeSC (P1, P2, and AY1 in Table I) at various kinetic order

TABLE I. Minimal Reaction Model for FeSC Biosynthesis in *S. cerevisiae*

Reaction[a]	Rate and modifiers[b]	Reaction[a]	Rate and modifiers[b]
IsuFe2S2 → Isu + 2 Fe	$v1 = \alpha_1 IsuFe2S2^{f11}$	AY1 → AY1_1	$v15 = \alpha_{15} AY1^{f151}$
IsuFe2S2 + Apo_P1 → P1 + Isu	$v2 = \alpha_2 IsuFe_2S_2^{f21}\ Apo\ P1^{f22}\ ([AY1])^{f23}$	→ Fe	$v16 = \alpha_{16}$
IsuFe2S2 + Apo_AY1 → Isu + Yah1	$v3 = \alpha_3 IsuFe_2S_2^{f31}\ Apo\_AY1^{f32}\ ([AY1])^{f33}$	Heme_Fe → Fe + Heme	$v_{17} = \alpha_{17} Heme\_Fe^{f171}$
IsuFe4S4 + Apo_P2 → P2 + Isu	$v4 = \alpha_4 IsuFe_4S_4^{f41}\ ApoP_2^{f42}\ ([AY1])^{f43}$	Fe →	$v18 = \alpha_{18} Fe^{f181}$
Isu + 2 Fe → IsuFe2S2	$v5 = \alpha_5 Isu^{f51} Fe^{f52}\ (Nfs_1^{f53}\ [AY1]^{f54})$	Heme + Fe → Heme_Fe	$v19 = \alpha_{19} Fe^{f191} Heme^{f192}$
IsuFe2S2 + 2 Fe → IsuFe4S4	$v6 = \alpha_6 IsuFe_2S_2^{f61} Fe^{f62}\ (Nfs_1^{f63}\ [AY1]^{f64})$	→ Heme	$v20 = \alpha_{20}\ (AY1)^{f201}$
IsuFe4S4 → IsuFe2S2 + 2 Fe	$v7 = \alpha_7 IsuFe_4S_4^{f71}$	Heme →	$v21 = \alpha_{21} Heme^{f211}$
P2_I → Apo_P2 + 4 Fe	$v8 = \alpha_8 P_2\_I^{f81}$	IsuFe2S2 + Apo_P2 → Isu + P2Fe2S2	$v22 = \alpha_{22} IsuFe_2S_2^{f221}\ ApoP_2^{f222}\ ([AY1])^{f223}$
P2_I → P2	$v9 = \alpha_9 P_2\_I^{f91} (Nfs_1^{f92}\ [AY1]^{f93})$	IsuFe2S2 + P2Fe2S2 → Isu + P2	$v23 = \alpha_{23} IsuFe_2S_2^{f231} P_2Fe_2S_2^{f232}\ ([AY1])^{f233}$
P2 → P2_I	$v10 = \alpha_{10} P_2^{f101}$	P2Fe2S2 → Apo_P2 + 2 Fe	$v24 = \alpha_{24} P_2Fe_2S_2^{f241}$
P1_I → Apo_P1 + 2 Fe	$v11 = \alpha_1 P_1\_I^{f111}$	IsuFe4S4 → Isu + 4 Fe	$v25 = \alpha_{25} IsuFe_4S_4^{f251}$
P1_I → P1	$v12 = \alpha_{12} P_1\_I^{f121}\ (Nfs_1^{f122}\ [AY1]^{f123})$	IsuFe2S2 → Isu + $FeSC_{cytoplasm}$	$v26 = \alpha_{26} IsuFe_2S_2^{f261}\ (AY1)^{f262}$
P1 → P1_I	$v13 = \alpha_{13} P_1^{f131}$	IsuFe4S4 → Isu + $FeSC_{cytoplasm}$	$v27 = \alpha_{27} IsuFe_4S_4^{f271}\ (AY1)^{f272}$
AY1_I → AY1	$v14 = \alpha_{14} AY1\_I^{f141}\ (Nfs_1^{f142}\ [AY1]^{f143})$	AY1_I → Apo_AY1 + 2 Fe	$v28 = \alpha_{28} AY1\_I^{f281}$

[a]Isu, scaffold for initial FeSC assembly; IsuFe2S2, IsuFe4S4, scaffold with a Fe2S2 and a Fe4S4 FeSC cluster assembled, respectively; Fe, mitochondrial iron; P1, generic enzyme needing a Fe2S2 FeSC to be functional; P2, generic enzyme needing a Fe4S4 FeSC to be functional; AY1, electron donor (either Arh1 or Yah1, depending on the experiment; see text for an explanation); Apo_P1, Apo_P2, Apo_AY1 -apo forms of P1, P2 and AY1 respectively; P1_1, P2_1, AY1_1-P1, P2 and AY1 forms with a damaged and repairable FeSC; P2Fe2S2 - P2 enzyme with an intermediate Fe2S2 cluster assembled; Heme, heme molecules synthesized in the mitochondrial matrix; Heme_Fe, heme molecules with iron.

[b]Species in parenthesis and brackets in the equations are not represented in the flux diagram, because they contribute to the catalysis of the reaction but are neither produced nor consumed in the reaction; bracketed species represent the scrutinized role of AY1.

TABLE II. Experiments to Determine the Effect of Arh1 and Yah1 on the Dynamical Behavior of the Network Upon Donation of Electrons to Different Subprocesses Within FeSC Synthesis[a]

Tested combination of subprocess(es) to which Arh1 or Yah1 can donate electrons in FeSC synthesis	Scanning intervals for the values of Arh1 or Yah1 kinetic orders in each of the subprocesses considered in FeSC synthesis							
	Synthesis		Transfer			Repair		
	$f54$	$f64$	$f23$	$f33$	$f43$	$f93$	$f123$	$f143$
Synthesis of FeSC (S)	$5 \geq f54 \geq 0$	$5 \geq f64 \geq 0$	$f23 = 0$	$f33 = 0$	$f43 = 0$	$f93 = 0$	$f123 = 0$	$f143 = 0$
Transfer of FeSC (T)	$f54 = 0$	$f64 = 0$	$5 \geq f23 \geq 0$	$5 \geq f33 \geq 0$	$5 \geq f43 \geq 0$	$f93 = 0$	$f123 = 0$	$f143 = 0$
Repair of FeSC (R)	$f54 = 0$	$f64 = 0$	$f23 = 0$	$f33 = 0$	$f43 = 0$	$5 \geq f93 \geq 0$	$5 \geq f123 \geq 0$	$5 \geq f143 \geq 0$
S and T	$5 \geq f54 \geq 0$	$5 \geq f64 \geq 0$	$5 \geq f23 \geq 0$	$5 \geq f33 \geq 0$	$5 \geq f43 \geq 0$	$f93 = 0$	$f123 = 0$	$f143 = 0$
S and R	$5 \geq f54 \geq 0$	$5 \geq f64 \geq 0$	$f23 = 0$	$f33 = 0$	$f43 = 0$	$5 \geq f93 \geq 0$	$5 \geq f123 \geq 0$	$5 \geq f143 \geq 0$
T and R	$f54 = 0$	$f64 = 0$	$5 \geq f23 \geq 0$	$5 \geq f33 \geq 0$	$5 \geq f43 \geq 0$	$5 \geq f93 \geq 0$	$5 \geq f123 \geq 0$	$5 \geq f143 \geq 0$
S, T, and R	$5 \geq f54 \geq 0$	$5 \geq f64 \geq 0$	$5 \geq f23 \geq 0$	$5 \geq f33 \geq 0$	$5 \geq f43 \geq 0$	$5 \geq f93 \geq 0$	$5 \geq f123 \geq 0$	$5 \geq f143 \geq 0$

[a]Each of these scans was done in three different models; (1) a model where only 4Fe-4S cluster transfer from scaffold proteins to 4Fe-4S apo-proteins was considered; (2) a model where only 2Fe-2S cluster transfer from scaffold proteins to 4Fe-4S apo-proteins was considered (i.e., a 4Fe-4S cluster built in two steps of transfer); (3) a model where 4Fe-4S clusters could assmeble in 4Fe-4S apo proteins via either (1) or (2). See Table III for details.

TABLE III. Experiments to Test the Different Possibilities for the Transfer and Assembly of 4Fe-4S Clusters in 4Fe-4S Apo-Proteins

Mode of FeSC assembly in 4Fe-4S apo-proteins	Values for the rate constants regulating each flux		
	4Fe-4S transfer flux	1st 2Fe-2S transfer flux	2nd 2Fe-2S transfer flux
2 transfer steps of 2Fe-2S cluster from scaffold	$\alpha_4 = 0$	$\alpha_{22} > 0$	$\alpha_{23} > 0$
1 transfer of 4Fe-4S cluster from scaffold	$\alpha_4 > 0$	$\alpha_{22} = 0$	$\alpha_{23} = 0$
2 transfer steps of 2Fe-2S cluster from scaffold or 1 transfer of 4Fe-4S cluster from scaffold	$\alpha_4 > 0$	$\alpha_{22} > 0$	$\alpha_{23} > 0$

values and at various ratios for the fluxes of the different processes shown in Table I. Details on how the scanning of parameters is performed are given in the appendix. The various modes of Arh1 or Yah1 action and the appropriate values for the Arh1 or Yah1 kinetic orders to be scanned for each of the modes are described in Table II and in the Appendix (Table AI), respectively.

Because the mechanism of transfer of a FeSC to 4Fe-4S apo-proteins is not clear, we tested the effects of Arh1 and Yah1 in all possible modes of 4Fe-4S cluster assembly in 4Fe-4S apo-proteins. How the different modes translate into parameter values is shown in Table III. The total amounts of 2Fe-2S–dependent enzymes, represented as P1 (P1 + Apo P1 + P1_I), and of 4Fe-4S–dependent enzymes P2 (P2 + Apo P2 + P2_I) are considered to be constant. This assumption is justified because protein synthesis and degradation usually takes place at a timescale (hours to days; approximately 20 h half-life for Arh1 and Yah1) that is orders of magnitude lower than that of FeSC turnover (minutes to hours).

The published data[15,16] that allow us to evaluate our models needs to be transformed for direct comparison with our simulations, so that iron levels and FeSC-dependent enzyme activity can be plotted against Yah1 levels. Because the transformation of the original data relies on image analysis of bands on a gel, which is inaccurate, the transformed data shown in Figure 2 can only be used as indicative of the correlation between active Yah1 levels and the activities of FeSC-dependent enzymes or the mitochondrial iron levels.

RESULTS

Structural Results

Arh1 is a soluble membrane-associated protein and Yah1 is a soluble protein. Maximal superposition of the backbone atoms between our model for Arh1 and the bovine homologue adrenodoxin reductase (AdR) shows a total deviation of 17.75 Å. Although this number is large, it is due mostly to the reconstructed loops, with the purpose of accommodating Arh1 residues that do not exist in the AdR. Before this reconstruction, the deviation is less than 6 Å, although gaps exist in the Arh1 model. Additionally, there is almost perfect sequence and structural residue conservation of the FADH and NAD(P) interacting residues between the two enzymes.[57,58] The only residue that is not conserved in the FADH binding site is the A17 of the bovine enzyme, which in the yeast Arh1 is S26, while the NAD(P) interacting residues Q153 and T373 in AdR are replaced by N177 and Q413, respectively in Arh1 (Table IV). Furthermore, the conserved residues that are involved in FAD and NAD(P) interactions can be almost perfectly superimposed in space, with a root-mean-square deviation (RMS) of less than 1 Å.

Yah1 and bovine adrenodoxin (Adx) are almost identical, with a total RMS of 4.51 Å between the backbone atoms of both structures after maximal alignment. A difference that is predicted from our model with respect to

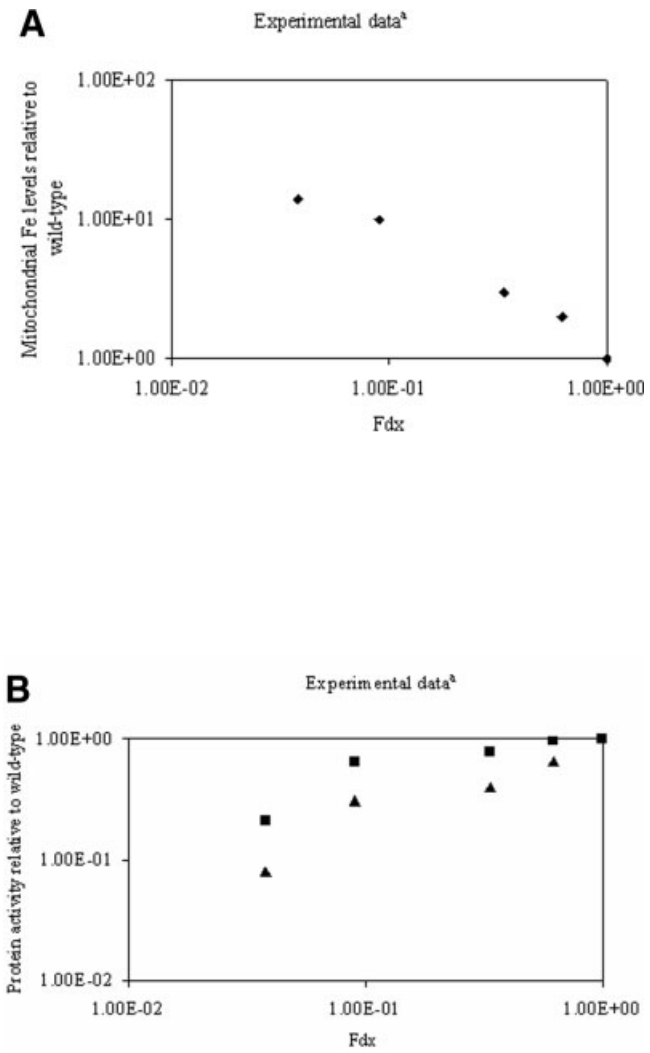

Fig. 2. Qualitative effect of varying gene expression of Arh1 or Yah1 (*x* axis) on mitochondrial iron accumulation and FeSC-dependent relative enzyme activities (*y* axis). Plots are dimensionless. Active Yah1 levels have been calculated assuming a first order decay of the concentration of Yah1 and fitting the data in Figures 2, 3, and 6 of Lange et al.[15] to this process. The decay constant is found to be approximately 0.045 h^{-1}. (**A**) Mitochondrial iron accumulation relative to the wild-type levels as a function of Yah1 degradation. (**B**) FeSC-dependent enzyme activities relative to the wild-type activity levels as a function of Yah1 degradation. Squares, succinate dehydrogenase activity; triangles, aconitase activity.

the mammalian Adx is the orientation of the putative binding site for the FeSC. Although model structures have a much lower definition than crystallographic or NMR structures, the difference in the spatial orientation of one of the 4 cysteines coordinating the FeSC between bovine and yeast ferredoxin is likely to be significant and not just an effect of model resolution. While in the yeast ferredoxin the 4 cysteine residues are within 10 residues of each other in the sequence, in the bovine ferredoxin, one of the cysteine residues is more than 50 residues away from the other 3 cysteines. Although the yeast cysteine does not superimpose with the bovine cysteine, it still allows for the coordination of an undistorted FeSC.

The crystallized bovine AdR–Adx complex[57] suggests that the interaction between the two molecules follows a lock–key model to a reasonable approximation [Fig. 3(A)]. As a control for our docking experiments, we uncoupled the bovine proteins and subjected them to the same docking procedure. We recovered a complex that is approximately the same as the crystallized complex. The predicted Arh1–Yah1 complex is also similar to the crystal [Fig. 3(A and 3B)]. Figure 4 (see Supplementary Table I) shows the surface residues in the interface between Arh1 and Yah1 that are less than 6 Å away from the opposing molecule.

The last 11 residues of Yah1 are predicted to act as physical anchors to the reductase, much in the same way the Adx tail acts in the known AdR–Adx complex. Although the overall electrostatic fields of the Yah1 molecular surface is negative, the Yah1 tail (Leu-Pro-Gln-Met-Thr-Arg-Asn-Val-Asn-Asn-Asn) is likely to be more positively charged than the adrenodoxin tail (Val-Pro-Asp-Ala-Val-Ser-Asp-Ala-Arg-Glu-Ser). The arrow in Figure 3(B) shows that there is a small negative patch of surface in the Arh1 molecule where the tail is anchored in the complex.

The minimal interprotein distance (< 7 Å) in the predicted Arh1–Yah1 complex allows for electron transfer between the two molecules.[59] Although our models have a lower resolution than actual structures, we use HARLEM to evaluate the maximal electron rates between the FADH molecule in the reductase and the FeSC of the substrate molecule. We have also explored possible structural explanations for why Adx is unable to rescue *yah1* mutations. We have calculated the best docking between Arh1 and Adx and between AdR and Yah1, which are similar to those shown in Figure 4(A and B). The maximum rate of electron transfer in the predicted Arh1–Adx complex is calculated to be one order of magnitude less than that for both the predicted complex Arh1–Yah1 and the Adx–AdR complex ($k_{\max Arh-Adx} = 6.3 \times 10^6$, $k_{\max Arh1-Yah1} = 1.2 \times 10^7$, $k_{\max AdxR-Adx} = 1.2 \times 10^7$, $k_{\max AdxR-Yah1} = 1.2 \times 10^7$). Point mutations in the residues predicted to be in the electron transfer pathway are predicted to modulate both the maximum rate of electron transfer and the pathway itself. This is also true for homologous point mutations in the AdR–Adx complex. The predicted maximum rate of electron transfer, in either the Arh1–Yah1 mutated complexes or the AdR–Adx mutated complexes, can increase or decrease, depending on the substituting amino acid. The change in the maximum rate of electron transfer is always found to be smaller than an order of magnitude.

We have perturbed the Arh1–Yah1 docking configuration to assess how that would affect the predictable maximal rate of electron transfer. Small rotations of Yah1 about the axis shown in Figure 3(A) cause little change in the maximal predictable rate of electron transfer between Arh1 and Yah1. However, as the rotation angle increases, the maximal predictable rate of electron transfer decreases and, for a rotation of Π radians, $k_{\max Arh1-Yah1} = 1.527 \times 10^{-3}$. Additionally, we have calculated maximal rates of electron transfer for the different complexes in the best docking cluster, and $k_{\max}$ is always orders of magnitude lower than that of the best complex. Thus, combining

our results with the available information regarding the AdR–Adx complex, we feel that there is good reason to admit that Yah1 is a substrate for Arh1, and that the later provides electrons for FeSC biogenesis through the former.

A Minimal Network Model for the Action of Arh1 and Yah1 on Mitochondrial Metabolism

Mounting evidence suggests the network of reactions shown in Table I as a minimal model for the coordinated action of the protein involved in FeSC biogenesis. A brief description of the reactions follows:

1. For reasons of simplicity, we considered only one electron donor species in our model (AY1, representing either Arh1 or Yah1 in Table I). This reproduces the published experimental set up, in which only the effect of either Arh1 or Yah1 is studied. If Arh1 acts on FeSC through Yah1, as appears to be the case, lumping the two molecules together does not change the qualitative results of our simulations. If Arh1 acts on FeSC biogenesis independently of Yah1, reactions $v3$, $v14$, $v15$, and $v28$ have rate constants equal to zero when scanning for Arh1 action (because Arh1 does not contain a FeSC) and different from zero when scanning for Yah1 action. Qualitatively, the results are similar in both cases.
2. Iron is imported into the mitochondrial matrix ($v16$). It is not consensual how Fe it is stored in the mitochondrial matrix. We assume as a simplification that a common mitochondrial iron pool is formed (Fe) and used for both heme A synthesis and for FeSC synthesis. We also consider a sink flux to account for any other usage or export of iron from the mitochondria ($v18$).
3. FeSC are thought to assemble initially in homodimers of the scaffold proteins, Isu1, Isu2, Isa1 Isa2, and probably Nfu1 in *S. cerevisiae*.[14,17,18,39,60] All these are lumped into one and represented by Isu. The FeSC assembly onto the dimer is catalyzed by the cysteine desulfurase Nfs1.[13,21,61] The dynamics of the cluster assembly into the scaffold are described by $v5$ (2Fe-2S cluster) and $v6$ (4Fe-4S cluster).
4. Once a 2Fe-2S FeSC is assembled in the scaffold, it can be transferred to 2Fe-2S apo-proteins,[62] represented by Apo_P1 and Apo_AY1 ($v2$ and $v3$, respectively). There is also the possibility that 2Fe-2S clusters are transferred to 4Fe-4S apo-proteins[62,63] ($v22$), represented by Apo_P2. A second 2Fe-2S transfer to P2Fe2S2 would lead to the formation of the appropriate 4Fe-4S FeSC on the apo-protein ($v23$).
5. If the FeSC remains on the scaffold proteins, it can convert over time into a 4Fe-4S FeSC[39] ($v6$), represented by IsuFe4S4.
6. Although there is no direct evidence of this, one cannot rule out the possibility that the 4Fe-4S FeSC can be transferred directly to 4Fe-4S apo-proteins ($v4$).
7. There is a natural turnover of FeSC, both in scaffold proteins and in the FeSC proteins ($v1$, $v7$, $v10$, $v13$, $v15$, and $v25$), for example, due to oxidative stress.[40] Proteins containing damaged FeSC are represented by P1_I, P2_I, and AY1_I. Nfs1 homologues reconstruct damaged FeSC directly in situ[40,64] ($v9$, $v12$, and $v14$). Alternatively, the damaged FeSC can be destroyed and lead to the formation of apo-proteins ($v8$, $v11$, and $v28$).
8. Finally, the FeSC can be transferred from the scaffold to the cytoplasm[13,24] ($v26$ and $v27$), affecting both, mitochondrial iron levels and FeSC dependent activity levels.
9. Arh1 and Yah1 are involved in the final steps of heme A synthesis (Heme), prior to the introduction of iron[16,26,29,31,32,35] ($v20$). Heme turnover is accounted for by $v21$. Alternative to being destroyed, Fe can be inserted into the heme molecule ($v19$), forming Heme_Fe. Turnover of this form of heme is also considered in our model ($v17$).
10. The involvement of Arh1 and Yah1 on FeSC is not well understood. We have described the possible modes of action of Arh1 and Yah1 previously.

These 10 steps define a minimal network model to study the action of Arh1 or Yah1 on mitochondrial FeSC assembly and iron metabolism. Most of the considered reactions exhibit nonlinear properties that make it impossible to predict the integrated behavior of the whole system intuitively.

To investigate the influence of the activity of Arh1 or Yah1 in the dynamical behavior of the network shown in Table I for every possible electron donation configuration from Arh1 or Yah1 to FeSC synthesis, we need to use nonlinear mathematical models. Our mathematical model

TABLE IV. Conservation of Protein Residues between Arh1 and Yah1

Bovine adrenodoxin reductase residues	Corresponding Arh1 residues	Cofactor binding the residues in the bovine enzyme
A17[a]	S26	FADH
E38[a]	E48	FADH
K39[a]	K49	FADH
L46[a]	L56	FADH
H55[a]	H65	FADH
R134[a]	R143	FADH
D159[a]	D183	FADH
W367[a]	W407	FADH
I376[a]	I416	FADH
T379[a]	T419	FADH
E209[b]	E235	NAD(P)
N155[b]	N179	NAD(P)
V156[b]	V180	NAD(P)
Q153[b]	N177	NAD(P)
R197[b]	R223	NAD(P)
R198[b]	R224	NAD(P)
S328[b]	S361	NAD(P)
Y331[b]	Y364	NAD(P)
T373[b]	Q413	NAD(P)
G374[b]	G414	NAD(P)

[a]Ziegler et al.[58]
[b]Ziegler and Schulz[57]

TABLE V. Simulating the Effect of Varying Arh1 or Yah1 Levels on Mitochondrial Iron Levels and on SDH and Aconitase Activities for Different Modes of Arh1 or Yah1 Action and Different Modes of 4Fe-4S Cluster Transfer: Comparison With Experimental Results[a]

Arh1 or Yah1 mode of action	4Fe-4S cluster mode of transfer to aconitase		
	Full 4Fe-4S cluster transfer and 2-step 2Fe-2S cluster transfer	Exclusive full 4Fe-4S cluster transfer	Exclusive 2-step 2Fe-2S cluster transfer
STR	Reproduces experimental results	Does not reproduce experimental results[e]	Reproduces experimental results
ST	Does not reproduce experimental results[e]	Does not reproduce experimental results[e]	Does not reproduce experimental results[e]
SR	Reproduces experimental results[b]	Does not Reproduce experimental results[e]	Reproduces experimental results[b]
TR	Reproduces experimental results[b]	Does not reproduce experimental results[e]	Reproduces experimental results[b]
S	Does not reproduce experimental results[c]	Does not Reproduce experimental results[e]	Does not reproduce experimental results[c]
T	Does not reproduce experimental results[c]	Does not reproduce experimental results[c]	Does not reproduce experimental results[c]
R	Does not reproduce experimental results[d]	Does not reproduce experimental results[c]	Does not reproduce experimental results[d]
	Does not reproduce experimental results[e]	Does not reproduce experimental results[e]	Does not reproduce experimental results[c]

[a]Reproduces experimental results, simulations show an inverse correlation between activity of the electron donor anf mitochondrial iron levels, as well as a direct correlation between electron donor levels and FeSC-dependent enzyme activity. Does not reproduce experimental results, simulations cannot reproduce at least one of the former correlations.
[b]For rates of FeSC transfer from the scaffold proteins to the FeSC apo-proteins at least one order of magnitude larger than the rate of FeSC synthesis on scaffold proteins.
[c]Mitochondrial iron levels increase upon decrease of Arh1 or Yah1 levels. SDH and aconitase activities either remain insensitive or increase with decreasing levels of Arh1 or Yah1.
[d]SDH and aconitase activities decrease upon decrease of Arh1 or Yah1 levels. Mitochondrial iron levels either remain insensitive or decrease with decreasing levels of Arh1 or Yah1.
[e]Mitochondrial iron levels either remain insensitive or decrease with decreasing levels of Arh1 or Yah1. SDH and aconitase activities either remain insensitive or increase with decreasing levels of Arh1 or Yah1.

is based on a well-established power law mathematical formalism.[65–67] The derivation of this model, as well as the mathematical model itself, is given in the Appendix.

The Role of Arh1 and Yah1 in Mitochondrial FeSC Assembly

The experimental depletion of Arh1 or Yah1[15,16] is reproduced in our models by decreasing the total amount of AY1 and solving the equations at the different levels of Arh1 or Yah1, followed by computing the steady-state percentage of each protein, P1, P2, and AY1, that is in its holo form, as well as the mitochondrial iron levels. It is assumed that FeSC-dependent enzyme activity is directly proportional to the percentage of P1 and P2 in holo forms. By working with normalized quantities and studying the steady-state or dynamical behavior of the model, we are able to determine the qualitative behavior that is most common to alternative network models. By changing the values for the kinetic orders of AY1 on the different equations, we determine the dynamical behavior of the system under all possible modes of action of Arh1 or Yah1 on FeSC synthesis. Although no clear data on the mechanism or accurate estimates for the parameter values of the system exist, using normalized quantities and the power law formalism as a modeling framework, we overcome these two concerns. Details on why this is so are given in the Appendix and in the references therein. Examples of how the use of this low-resolution modeling approach has assisted in discerning between alternative roles of proteins in different cellular networks can be found in the literature.[68,69]

Tables II and III describe the various kinetic experiments and explain the nomenclature for the each possible mode of action of AY1.

A qualitative description of the ability of our model to reproduce the experimental results is shown in Table V. Our simulations show a decrease in heme levels as the activity of AY1 decreases for all modes of AY1 action, which concurs with the observed experimental result[15,16,26,29,70] and is therefore of no assistance in distinguishing between alternative networks. Table V discriminates the effect of varying AY1 levels on mitochondrial iron accumulation and FeSC-dependent enzyme activity according to different AY1 modes of action. It further discriminates, for each mode of AY1 action, the effect of varying AY1 on the mitochondrial iron levels and on the activity of FeSC-dependent enzymes, according to the different possible modes of transfer of 4Fe-4S cluster to P2 (i.e., allowing only the full 4Fe-4S cluster to be transferred, allowing only a two-step transfer of 2Fe-2S clusters, and allowing for both mechanism of transfer to coexist).

Only the STR mode of action in Table II can qualitatively reproduce the previously described[15,16] mitochondrial iron accumulation and the decrease in FeSC-dependent enzyme activity caused by AY1 depletion over all tested parameter values. SR and TR electron transfer modes can reproduce the same experiments as long as the basal relative rate of FeSC transfer from the scaffold

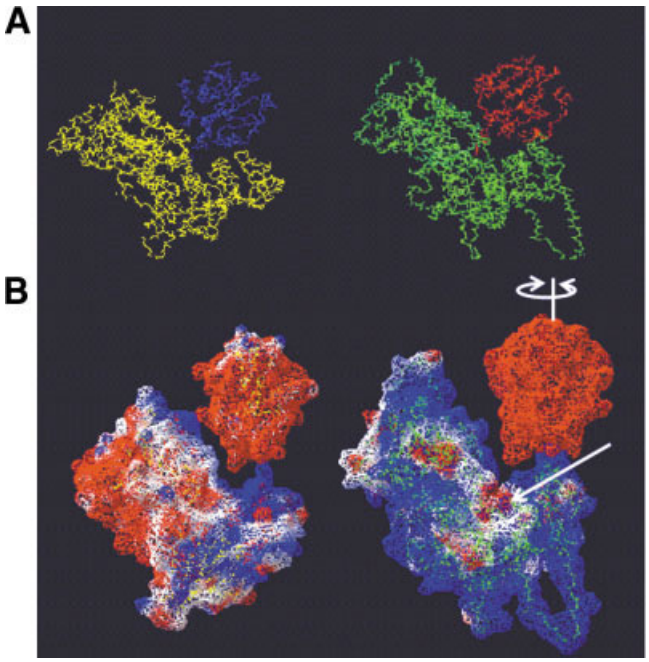

Fig. 3. Complex between ferredoxin (blue) and ferredoxin reductase (yellow). (**A**) Complex on the left is the one that was crystallized for bovine adrenodoxin and adrenodoxin reductase. Complex on the right is the one predicted from our structural models of Arh1 and Yah1. (**B**) Left, bovine complex; right, yeast complex. The electrostatic potential have been calculated assuming a protein dielectric constant of 4, a solvent dielectric constant of 80, and a solvent ionic strength of 0.1 *M*. Residues with a surface charge calculated to be larger than 1.8 are colored blue. Residues with a surface charge calculated to be smaller than −1.8 are colored red. Remaining residues are in white. The ferredoxin surface that docks the reductase is highly negative (red) and binds a pocket of positive residues (blue). The white arrow indicates the surface patch where mutation of three Arg residues into Asp residues is predicted to disrupt Arh1–Yah1 interaction.

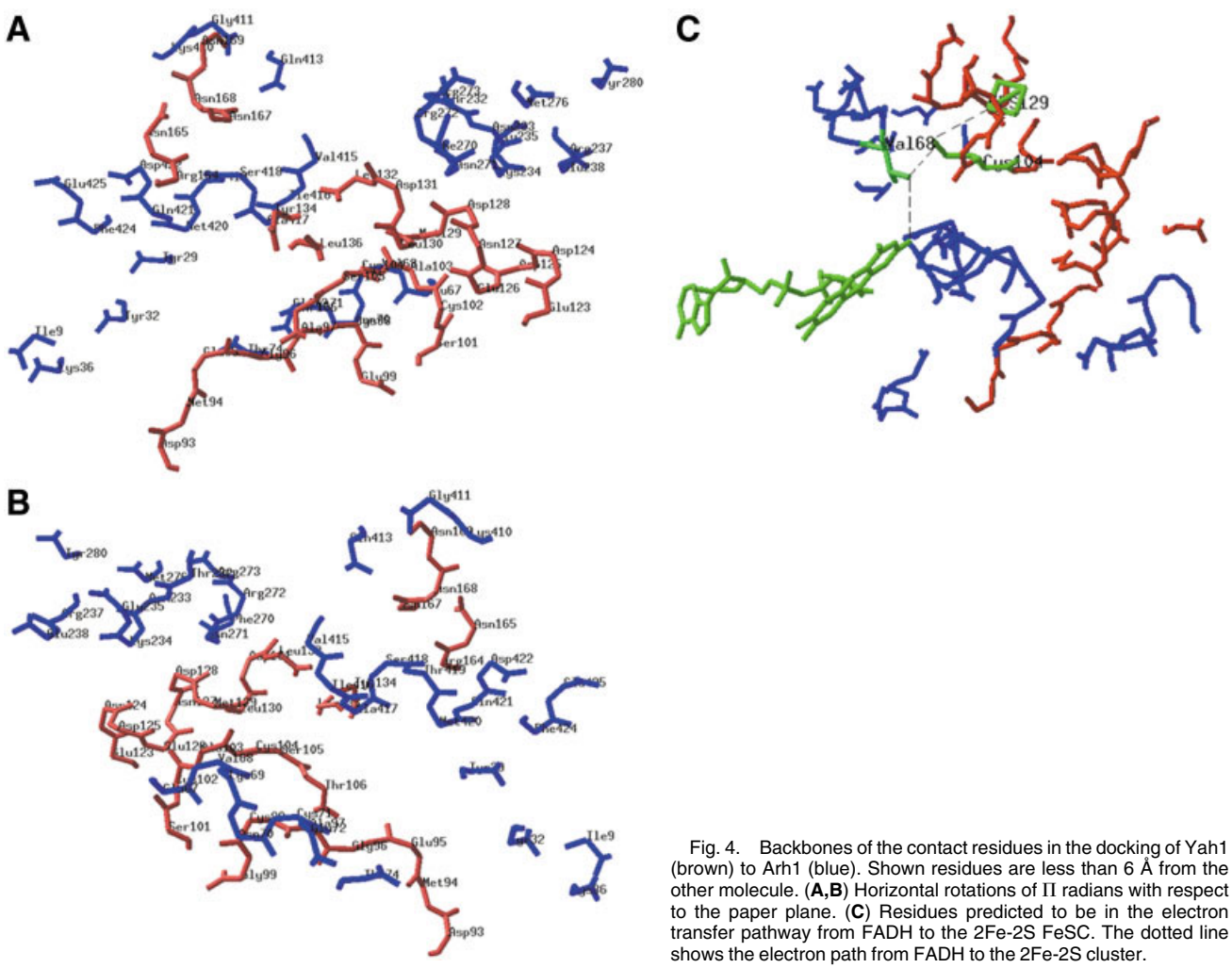

Fig. 4. Backbones of the contact residues in the docking of Yah1 (brown) to Arh1 (blue). Shown residues are less than 6 Å from the other molecule. (**A,B**) Horizontal rotations of Π radians with respect to the paper plane. (**C**) Residues predicted to be in the electron transfer pathway from FADH to the 2Fe-2S FeSC. The dotted line shows the electron path from FADH to the 2Fe-2S cluster.

proteins to the FeSC apo-proteins is at least one order of magnitude larger than the rate of FeSC synthesis on scaffold proteins. Previous interpretation of the experimental results downplayed the importance of Arh1 or Yah1 electron transfer at the repair stage of mitochondrial FeSC metabolism, because it was assumed that proteins with damaged FeSCs did not retain iron ions to sustain Nfs1 action.[15]

DISCUSSION

In this work, we combine structural modeling with protein docking of model structures to obtain structural models of Arh1 and Yah1, and predict the best docking mode between the two molecules. We find that the predicted best complex between Yah1 and Arh1 is very similar in spatial orientation to the experimentally determined complex between bovine Adx and AdR. Furthermore, although the sequence identity between Arh1 and bovine Adx is 33.9% (similarity 50.3%), there is almost total sequence and spatial conservation of the residues that bind NADP and FADH in AdR and the presumptive NADP(H) and FADH binding residues in Arh1. All our structural data, interpreted in light of the known Adx–AdR complex, suggest that Arh1 can indeed be the reductase for Yah1.

Mutations in the Yah1 C-terminal are predicted to perturb the docking between Arh1 and Yah1, as well as the maximal electron transfer rate between the two molecules. Additionally point mutations of residues Arg268, Arg272, and Arg273 to Asp residues may destroy potential salt bridges between Arh1 and Yah1, by analogy with the AdR–Adx complex.[71] With that, the interaction between the two proteins may be disturbed. If this is so, Yah1 would become a poorer substrate for Arh1 and potentially mimic the effects of decreasing the levels of *arh1* or *yah1* gene expression on FeSC-dependent enzyme activities and on mitochondrial iron accumulation. When done *in silico,* any combination of the proposed Arg to Asp point mutations (including double and triple mutations) has little effect in changing the best docking complex that is predicted between Arh1 and Yah1. However, homologous mutations in AdR have a similarly small effect on the predicted docking between AdR and Adx, although they are known to form salt bridges that stabilize the crystallized complex. A repetition of the experiments reported by Lange et al.[15] and by Li et al.[72] using the mutated forms of Yah1 or Arh1 would be a way to test the possible Arh1–Yah1 interaction.

Several processes have been proposed as the target for Arh–Yah1 electrons in FeSC biosynthesis, namely, (1) import of reduced iron to the mitochondrial matrix, (2) initial FeSC assembly in the scaffolds, (3) transfer of the FeSC from the scaffolds to the apo-proteins, or (4) in situ repair of damaged FeSC.[15,73] Experimental results exclude possibility (1).[36] Our own dynamical modeling results agree with the experimental results because, if (1) was the destination of Yah1 electrons, mitochondrial iron levels would decrease upon depletion of Arh1 or Yah1 (data not shown), which is contrary to the observed experimental results.[15,16,36]

A direct correlation observed to occur between the iron contents of immunoprecipitated mitochondrial FeSC-dependent proteins and Yah1 levels[15] has been interpreted as indicating that Yah1 acts mostly on de novo FeSC synthesis.[15] This interpretation rests upon several assumptions that are not fully justified, the two most relevant ones being:

1. It assumes that damaged FeSC's do not retain iron. However, it has been shown that, at least for bacterial proteins, some damaged FeSC's retain iron ions.[40]
2. It assumes that a decrease in the iron contents of FeSC proteins can only ensue from defective de novo FeSC synthesis. Yet the decrease in iron levels can also ensue from decreased in situ repair of FeSC, which allows damaged FeSC's to release their iron ions before being repaired.

Our results suggest that Yah1 (Arh1) electron donation to the repair of FeSC clusters is fundamental for the correlation between Yah1 (Arh1) levels and FeSC-dependent enzyme activity or mitochondrial iron levels. If Yah1 (Arh1) does not donate electrons for FeSC repair, the model is unable to reproduce the correlations. The results shown in Table V suggest that the effect of Yah1 (Arh1) on mitochondrial iron levels is most likely due to electrons donated to the synthesis stage of FeSC. When an S mode of action of Yah1 (Arh1) is considered, mitochondrial iron accumulates as Yah1 (Arh1) activity decreases, while FeSC-dependent enzyme activity is mostly independent of Arh1 or Yah1 levels. Similarly, our simulations suggest that electron donation of Yah1 (Arh1) to the in situ repair of FeSC clusters is likely to be responsible, in large part, for the inverse correlation between Yah1 (Arh1) levels and FeSC-dependent enzyme activity.

Our simulations exclude that only transfer of 4Fe-4S cluster from FeSC scaffold proteins to 4Fe-4S–dependent apo-proteins takes place. There must be at least some 2Fe-2S transfer to reproduce the experimental correlation between Yah1 (Arh1) levels and FeSC-dependent enzyme activity. Nevertheless, we cannot distinguish between an exclusive 2Fe-2S transfer and mixed transfer of 2Fe-2S and 4Fe-4S clusters.

In summary, our results emphasize the importance of electrons donation for the in situ FeSC repair process. Previous interpretations of the experimental results based solely on linear cause–effect reasoning discarded this possibility. Thus, the modeling results emphasize the importance of using mathematical models and a systems biology perspective when interpreting results in experiments involving nonlinear systems.

ACKNOWLEDGMENTS

We thank Drs. Pedro Echave, Monica Sousa, Armindo Salvador and two anonymous referees for suggestions that greatly improved the quality and clarity of this article.

REFERENCES

1. Beinert H, Holm RH, Munck E. Iron-sulphur clusters: Nature's modular, multipurpose structures. Science 1997;277:653–659.

2. Frazzon J, Fick JR, Dean DR. Biosynthesis of iron–sulphur clusters is a complex and highly conserved process. Biochem Soc Trans 2002;30:680–685.
3. Kiley PJ, Beinert H. The role of Fe-S proteins in sensing and regulation in bacteria. Curr Opin Microbiol 2003;6:181–185.
4. Rees DC. Great metalloclusters in enzymology. Ann Rev Biochem 2002;71:221–246.
5. Rees DC, Howard JB. The interface between the biological and inorganic worlds: iron–sulfur metalloclusters. Science 2003;300: 929–931.
6. Rodriguez-Manzaneque, MT, Tamarit J, Belli G, Ros J, Herrero, E. Grx5 is a mitochondrial glutaredoxin required for the activity of iron/sulfur enzymes. Mol Biol Cell 2002;13:1109–1121.
7. Kim R, Saxena S, Gordon DM, Pain D, Dancis A. J-domain protein, Jac1p, of yeast mitochondria required for iron homeostasis and activity of Fe-S cluster proteins. J Biol Chem 2001;276: 17524–17532.
8. Lutz T, Westermann B, Neupert W, Herrmann JM. The mitochondrial proteins Ssq1 and Jac1 are required for the assembly of iron sulfur clusters in mitochondria. J Mol Biol 2001;307:815–825.
9. Schilke B, Voisine C, Beinert H, Craig, E. Evidence for a conserved system for iron metabolism in the mitochondria of *Saccharomyces cerevisiae*. Proc Natl Acad Sci USA 1999;96:10206–10211.
10. Voos W, Röttgers K. Molecular chaperones as essential mediators of mitochondrial biogenesis. Biochim Biophys Acta 2002;1592:51–62.
11. Voisine C, Cheng YC, Ohlson M, Schilke B, Hoff K, Beinert H, Marszalek J, Craig EA. Jac1, a mitochondrial J-type chaperone, is involved in the biogenesis of Fe/S clusters in *Saccharomyces cerevisiae*. Proc Natl Acad Sci USA 2001;98:1483–1488.
12. Kispal G, Csere P, Guiard B, Lill R. The ABC transporter Atm1p is required for mitochondrial iron homeostasis. FEBS Lett 1998;418: 346–350.
13. Kispal G, Csere P, Prohl C, Lill R. The mitochondrial proteins Atm1p and Nfs1p are essential for biogenesis of cytosolic Fe/S proteins. EMBO J 1999;18:3981–3989.
14. Mühlenhoff U, Richhardt N, Gerber J, Lill R. Characterization of iron–sulfur protein assembly in isolated mitochondria: a requirement for ATP, NADH, and reduced iron. J Biol Chem 2002;277: 29810–29816.
15. Lange H, Kaut A, Kispal G, Lill R. A mitochondrial ferredoxin is essential for biogenesis of cellular iron–sulfur proteins. Proc Natl Acad Sci USA 2000;97:1050–1055.
16. Li J, Saxena S, Pain D, Dancis A. Adrenodoxin reductase homologue (Arh1p) of yeast mitochondria required for iron homeostasis. J Biol Chem 2001;276:1503–1509.
17. Garland SA, Hoff K, Vickery LE. Culotta V. C. *Saccharomyces cerevisiae* ISU1 and ISU2, members of a well-conserved gene family for iron–sulfur cluster assembly. J Mol Biol 2000;294:897–907.
18. Jensen LT, Culotta VC. Role of *Saccharomyces cerevisiae* ISA1 and ISA2 in iron homeostasis. Mol Cell Biol 2000;20:3918–3927.
19. Kaut A, Lange H, Diekert K, Kispal G, Lill R. Isa1p is a component of the mitochondrial machinery for maturation of cellular iron–sulfur proteins and requires conserved cysteine residues for function. J Biol Chem 2000;275:15955–15961.
20. Pelzer W, Mühlenhoff U, Diekert K, Siegmund K, Kispal G, Lill R. Mitochondrial Isa2p plays a crucial role in the maturation of cellular iron–sulfur proteins. FEBS Lett 2000;476:134–139.
21. Li J, Kogan M, Knight SA, Pain D, Dancis A. Yeast mitochondrial protein, Nfs1p, coordinately regulates iron–sulfur cluster proteins, cellular iron uptake, and iron distribution. J Biol Chem 2000;274:33025–33034.
22. Duby G, Foury F, Ramazzotti A, Herrmann J, Lutz T. A non-essential function for yeast frataxin in iron-sulfur cluster assembly. Hum Mol Genet 2002;11:2635–2643.
23. Mühlenhoff U, Richhardt N, Ristow M, Kispal G, Lill R. The yeast frataxin homolog Yfh1p plays a specific role in the maturation of cellular Fe/S proteins. Hum Mol Genet 2002;11:2025–2036.
24. Lange H, Lisowsky T, Gerber J, Mühlenhoff U, Kispal G, Lill R. An essential function of the mitochondrial sulphydryl oxidase Erv1p/ALR in the maturation of cytosolic Fe/S proteins. EMBO Rep 2001;2:715–720.
25. Pandolfo M. The molecular basis of Friedreich ataxia. Adv Exp Med Biol 2002;516:99–118.
26. Manzella L, Barros MH, Nobrega FG. ARH1 of *Saccharomyces cerevisiae*, a new essential gene that codes for a protein homologous to the human adrenodoxin reductase. Yeast 1998;14:839–846.
27. Lacour T, Aschtetter T, Dumas B. Characterization of recombinant adrenodoxin reductase homologue (Arh1p) from yeast: Implications in in vitro cytochrome P45011 monooxygenase system. J Biol Chem 1998;273:23984–23992.
28. Manzella L, Barros MH, Nobrega FG. ARH1 of *Saccharomyces cerevisiae*, a new essential gene that codes for a protein homologous to the human adrenodoxin reductase. Yeast 1998;14:839–846.
29. Barros MH, Nobrega FG. YAH1 of *Saccharomyces cerevisiae*, a new essential gene that codes for a protein homologous to human adrenodoxin. Gene 1999;233:197–203.
30. Uetz P. Two-hybrid arrays. Curr Opin Chem Biol 2002;6:57–62.
31. Barros MH, Tzagoloff A. Regulation of heme A biosynthetic pathway in *Saccharomyces cerevisiae*. FEBS Lett 2002;516:119–123.
32. Barros MH, Carlson CG, Glerum DM, Tzagoloff A. Involvement of mitochondrial ferredoxin and Cox15p in hydroxylation of heme O. FEBS Lett 2001;492:133–138.
33. Zhang L, Hach A. Molecular mechanism of heme signaling in yeast: the transcriptional activator Hap1 serves as the key mediator. Cell Mol Life Sci 2001;56:415–426.
34. Zheng L, Cash VL, Flint DH, Dean DR. Assembly of iron-sulfur clusters, Identification of an *iscSUA-hscBA-fdx* gene cluster from *Azotobacter vinelandii*. J Biol Chem 1998;273:13264–13272.
35. Barros MH, Nobrega F, Tzagoloff A. Mitochondrial ferredoxin is required for heme A synthesis in *Saccharomyces cerevisiae*. J Biol Chem 2002;277:9997–10002.
36. Lange H, Kyspal G, Lill R. Mechanism of iron transport to the site of heme synthesis inside yeast mitochondria. J Biol Chem 1999;274: 18989–8996.
37. Lill R, Kispal G. Maturation of cellular Fe-S proteins, an essential function of mitochondria. Trends Biochem Sci 2000;25:352–356.
38. Mühlenhoff U, Lill R. Biogenesis of iron–sulfur proteins in eukaryotes, a novel task of mitochondria that is inherited from bacteria. Biochim Biophys Acta 2000;1459:370–382.
39. Agar JN, Krebs C, Frazzon J, Huynh BH, Dean DR, Johnson MK. IscU as a scaffold for iron–sulfur cluster biosynthesis: sequential assembly of (2Fe-2S) and (4Fe-4S) clusters in IscU. Biochemistry 2000;39:7856–7862.
40. Yang W, Rogers PA, Ding H. Repair of nitric oxide-modified ferredoxin (2Fe-2S) cluster by cystein desulfurase (ISCS). J Biol Chem 2002;277:12868–12872.
41. Moult J, Fidelis K, Zemla A, Hubbard T. Critical assessment of methods of protein structure prediction (CASP), round IV. Proteins 2002;45:2–7.
42. See also http://predictioncenter.llnl.gov/casp5/pubresults/casp_browser/.
43. Bates PA, Kelley LA, MacCallum RM, Sternberg MJE. Enhancement of protein modelling by human intervention in applying the automatic programs 3D-JIGSAW and 3D-PSSM. Proteins 2001;45: 39–46.
44. Guex N, Peitsch MC. SWISS-MODEL and the Swiss-PdbViewer: an environment for comparative protein modeling. Electrophoresis 1997;18:2714–2723.
45. Schwede T, Diemand A, Guex N, Peitsch MC. Protein structure computing in the genomic era. Res Microbiol 2000;151:107–112.
46. Thompson JD, Higgins DG, Gibson TJ. CLUSTAL W: improving the sensitivity of progressive multiple sequence alignment through sequence weighting, position-specific gap penalties and weight matrix choice. Nucleic Acids Res 1994;22:4673–4680.
47. Brocchieri L, Karlin S. A symmetric-iterated multiple alignment of protein sequences. J Mol Biol 1998;276:249–264.
48. Westbrook J, Feng Z, Chen L, Yang H, Berman HM. The Protein Data Bank and structural genomics. Nucleic Acids Res 2003;31: 489–491.
49. Weiner SJ, Kollman PA, Case DA, Singh UC, Ghio C, Alagona G, Profeta S, Weiner PK. A new force field for molecular mechanical simulation of nucleic acids proteins. J Am Chem Soc 1984;106:765–784.
50. Halperin I, Buyong M, Wolfson H, Nussinov R. Principles of docking: an overview of search algorithms and a guide to scoring functions. Proteins 2002;47:409–443.
51. Smith GR, Sternberg MJE. Prediction of protein–protein interactions by docking methods. Curr Opin Struct Biol 2002;12:28–35.

52. Tovchigrechko A, Wells CA, Vakser IA. Docking of protein models. Protein Sci 2002;11:1888–1896.
53. Vakser IA. Low-resolution docking, prediction of complexes for undetermined structures. Biopolymers 1996;39:455–464.
54. Vakser IA. Evaluation of GRAMM low-resolution docking methodology on hemaglutin–antibody complex. Proteins 1997;29:226–230.
55. Beratan DN, Betts JN, Onuchic JN. Protein electron transfer rates set by the bridging secondary and tertiary structure. Science 1991;252:1285–1288.
56. See also http://www.kurnikov.org/harlem_main.html for download.
57. Ziegler GA, Schulz GE. Crystal structures of adrenodoxin reductase in complex with NADP+ and NADPH suggesting a mechanism for the electron transfer of an enzyme family. Biochemistry 2000;39:10986–10995.
58. Ziegler GA, Vonrhein C, Hanokoglu I, Schulz GE. The structure of adrenodoxin reductase of mitochondrial P450 systems: electron transfer for steroid biosynthesis. J Mol Biol 1999; 289:981–990.
59. Page CC, Moser CM, Chen X, Dutton PL. Natural engineering principles of electron tunneling in biological oxidation–reduction. Nature 1999;402:47–52.
60. Agar JN, Yuvaniyama P, Jack RF, Cash VL, Smith AD, Dean DR, Johnson MK. Modular organization and identification of a mononuclear iron-binding site within the NifU protein. J Biol Inorg Chem 2000;5:167–177.
61. Urbina HD, Silberg JJ, Hoff KG, Vickery LE. Transfer of sulfur from IscS to IscU during FeandS cluster assembly. J Biol Chem 2001;276:44521–44526.
62. Nishio K, Nakay M. Transfer of iron sulfur cluster from nifU to apoferredoxin. J Biol Chem 2000;275:22615–22618.
63. Wollenberg M, Berndt C, Bill E, Schwenn JD, Seidler A. A dimer of the FeSC cluster biosynthesis protein IscA from cyanobacteria binds a (2Fe2S) cluster between two protomers and transfers it to (2Fe2S) and (4Fe4S) apo-proteins. Eur J Biochem 2003;270:1662–1671.
64. Bui BTS, Escalettes F, Chottard G, Florentin D, Marquet A. Enzyme-mediated sulfide production for the reconstitution of (2Fe-2S) clusters into apo-biotin synthase of *Escherichia coli* sulfide transfer from cysteine to biotin. Eur J Biochem 2000;267:2688–2694.
65. Alves R, Savageau M. A comparative analysis of prototype two-component systems with either bifunctional or monofunctional sensors: differences in molecular structure and physiological function. Mol Microbiol 2003;48:25–51.
66. Savageau MA. Biochemical systems analysis II: The steady state solution for an *n*-pool system using a power law approximation. J Theor Biol 1969;25:370–379.
67. Shiraishi F, Savageau MA. The tricarboxylic acid cyclein *Dyctiostelium discoideum*: II. Evaluation of model consistency and robustness. J Biol Chem 1992;267:22919–22925.
68. Alves R, Savageau MA. Extending the method of mathematically controlled comparison to include numerical comparisons. Bioinformatics 2000;16:786–798.
69. Battogtokh D, Asch DK, Case ME, Arnold J, Schuttler HB. An ensemble method for identifying regulatory circuits with special reference to the *qa* gene cluster of *Neurospora crassa*. Proc Natl Acad Sci USA 2002;99:16904–16909.
70. Lacour T, Aschtetter T, Dumas B. Characterization of recombinant adrenodoxin reductase homologue (Arh1p) from yeast: implications in in vitro cytochrome P45011 monooxygenase system. J Biol Chem 1998;273:23984–23992.
71. Ziegler GA, Schulz GE. Crystal structures of adrenodoxin reductase in complex with NADP+ and NADPH suggesting a mechanism for the electron transfer of an enzyme family. Biochemistry 2000;39:10986–10995.
72. Li J, Saxena S, Pain D, Dancis A. Adrenodoxin reductase homologue (Arh1p) of yeast mitochondria required for iron homeostasis. J Biol Chem 2001;276:1503–1509.
73. Wu SP, Wu G, Surerus KK, Cowan JA. Iron-sulfur cluster biosynthesis: kinetic analysis of (2Fe-2S) cluster transfer from holo ISU to apo Fd: role of redox chemistry and a conserved aspartate. Biochemistry 2002;41:8876–8885.
74. Voit EO, Savageau MA. Accuracy of alternative representations for integrated biochemical systems. Biochemistry 1987;26:6869–6880.
75. Voit EO, Ferreira AEN. Computational analysis of biochemical systems: a practical guide for biochemists and molecular biologists. Cambridge University Press: Cambridge, UK, 2000.
76. Mendes P. Biochemistry by numbers: simulation of biochemical pathways with Gepasi 3. Trends Biochem Sci 1998;22:361–363.
77. Foury F, Roganti T. Deletion of the mitochondrial carrier genes MRS3 and MRS4 suppresses mitochondrial iron accumulation in a yeast frataxin-deficient strain. J Biol Chem 2002;277:24475–24483.
78. Gordon DM, Kogan M, Knight SA, Dancis A, Pain D. Distinct roles for two N-terminal cleaved domains in mitochondrial import of the yeast frataxin homolog, Yfh1p. Hum Mol Genet 2001;10:259–269.
79. Cowan JA, Chen CA. Characterization of the soluble domain of the ABC7 type transporter Atm1. J Biol Chem 2004. Forthcoming.
80. Brown NM, Anderson SA, Steffen DW, Carpenter TB, Kennedy MC, Walden WE, Eisenstein RS. Novel role of phosphorylation in Fe-S cluster stability revealed by phosphomimetic mutations at Ser-138 of iron regulatory protein 1. Proc Natl Acad Sci USA 1998;95:15235–15240.
81. Brown NM, Kennedy MC, Antholine WE, Eisenstein RS, Walden WE. Detection of a [3Fe-4S] cluster intermediate of cytosolic aconitase in yeast expressing iron regulatory protein 1: insights into the mechanism of Fe-S cluster cycling. J Biol Chem 2002;277:7246–7254.
82. Varghese S, Tang Y, Imlay JA. Contrasting sensitivities of *Escherichia coli* aconitases A and B to oxidation and iron depletion. J Bacteriol 2003;185:221–230.

APPENDIX: DERIVATION OF THE MATHEMATICAL MODEL AND PARAMETER SCANNING PROCEDURE

Mathematical Derivation

Two types of approximations were used to derive the equations for Table I:

1. To simplify the model, in several cases, various reactions and processes were lumped together in one flux. This is the case, for example, of the heme A synthesis or the FeSC assembly at the scaffold proteins.
2. Because the exact mathematical form of the rate expressions is unknown, they were approximated using the power law equations.[65–67] This formalism is able to describe an unknown target function around an operating point by using a Taylor series in logarithmic space.[66,74]

We derive the power law equations that describe the dynamical behavior of each of the molecular species of interest as follows:

1. Consider a molecular species of interest, for example, heme, in Table I. The dynamical behavior of this species results from the balance of different reactions: (a) The flux corresponding to the lumped processes prior to heme A synthesis ($v20$ in Table I); (b) the flux accounting for the decrease in free heme levels caused by iron insertion ($v19$ in Table I); and (c) the flux accounting for the aggregated processes of heme A depletion ($v21$ in Table I). Although $v20$ is a function of many intermediate metabolites and enzymes, we are only interested in the role of Arh1 and Yah1. Thus, we will assume that the other metabolites and enzymes remain at approximately constant levels, which is the same assumption that is made during the wet lab inhibition of Arh1 or Yah1 gene expression. Similar assumptions are made for fluxes $v19$ and $v21$, and the resulting equations that

account for the time evolution of the heme pool is

$$d\,Heme/dt = v_{20}\,(AY1) - v_{19}\,(Heme, Fe) - v_{21}\,(Heme) \quad \text{(A1)}$$

2. For each flux, we now write a power law description, with as many terms as the number of species on which the flux is considered to be dependent, multiplied by a rate constant. For example, the power law that describes the flux $v20$ is $\alpha_{20}\,(AY1)^{f201}$. $\alpha 20$ is a multiplicative parameter that includes all effectors that are considered to be constant and it can be derived mathematically from Eq. (A1) by the formula $\alpha_{20} = (v_{20}\,(AY1)^{-f_{201}})|_0$, where the subindex 0 indicates the operating point for the derivation procedure. The exponent f_{201} is an apparent kinetic order of the flux $v20$ with respect to $AY1$ and is given by

$$f_{201} = [d\ \mathrm{Log}\ v_{20}/d\mathrm{Log}\ (AY1)]|_0 = [(AY1)/v_{20}]|_0[dv_{20}/d\ (AY1)]|_0\,,$$

where the subindex 0 indicates the operating point for the derivation procedure. Finally, the full power law representation for the dynamic behavior of Heme in our model is

$$dHeme/dt = \alpha_{20}\,(AY1)^{f_{201}} - \alpha_{19} Fe^{f_{191}} Heme^{f_{192}} - \alpha_{21} Heme^{f_{211}}. \quad \text{(A2)}$$

In order to write the complete set of equations for the network shown in Table I, we only need to repeat this procedure for each molecular species in the network. The resulting mathematical model is a set of ordinary differential equations in GMA (generalized mass action) form. The multiplicative parameters α_i are rate constants, while the exponential parameters or kinetic orders (f_{ij}) represent the strength of the direct influence of a given molecular species on a given flux. If there is no direct influence of species j on flux i, then $f_{ij} = 0$. If species j positively modulates or is a substrate of flux i, then $f_{ij} > 0$. If species j negatively modulates or inhibits flux i, then $f_{ij} < 0$. This mathematical approximation is guaranteed to be accurate within a given range about the operating point.[66]

The system of ordinary differential equations (SODE) that represents the network in Table I is the following:

$$dIsu/dt = v1 + v2 + v3 + v4 + v22 + v23 + v25 + v26 + v27 - v5$$
$$dIsu\mathrm{Fe_2S_2}/dt = v5 + v7 - v\ 1 - v2 - v3 - v6 - v22 - v23 - v26$$
$$dIsu\mathrm{Fe_4S_4}/dt = v6 - v4 - v7 - v25 - v27$$
$$dApo\ P2/dt = v8 + v24 - v4 - v22$$
$$dP2\mathrm{Fe_2S_2}/dt = v22 - v23 - v24$$
$$dp2/dt = v4 + v9 + v23 - v10$$
$$dP2\_I/dt = -\,dApo\ P2/dt - dP2/dt - dP2\mathrm{Fe2S2}/dt$$
$$dApo\ P1/dt = v11 - v2$$
$$dP1/dt = v2 + v12 - v13$$
$$dP1\_I/dt = -\,dApo\ P1/dt - dP1/dt$$
$$dApo\_AY1/dt = v28 - v3$$
$$dAY1/dt = v3 + v4 - v15$$
$$dAY\_I/dt = -dApo\_AY1/dt - dAY1/dt$$
$$dFe/dt = v16 + v17 + 2(v1 + v7 + v11 + v24 + v28) + 4(v8 + v25) - v18 - v19 - 2(v5 + v6)$$
$$dHeme/dt = v17 + v20 - v19 - v21$$
$$dHeme\_\mathrm{Fe}/dt = v19 - v17$$

Each vi ($1 \le i \le 28$) is given in detail in Table I. Numerical solution of SODE in our work has been done using the programs PLAS[75] and GEPASI.[76]

TABLE AI. Parameter Constraints and Parameter Values[a]

Rate constant constraints	Kinetic orders constraints
$\alpha 1 = \alpha 7 = 0.05$	$f11 = f71 = f81 = f111 = f241 = f251 = f281 = 1$
$\alpha 2 = \alpha 3 = \alpha 4 = \alpha 22 = \alpha 23 = 0.1$	$f21 = f31 = f41 = f221 = f231 = 1$
$\alpha 5 = \alpha 6 = 0.05$	$f22 = f32 = f42 = f222 = f232 = 1$
	$0 \le f23 = f33 = f43 = f223 = f233 \le 5$
$\alpha 8 = \alpha 11 = \alpha 28 = \alpha 24 = \frac{\alpha 25}{2} = 0.05$	$f51 = f61 = 0.5$
$\alpha 10 = \alpha 13 = \alpha 15 = 0.05$	$f52 = f62 = 0.5$
$0.001 \le \alpha 9 = \alpha 12 = \alpha 14 \le 100$	$f53 = f63 = 1$
$\alpha 16 = 0.1$	$0 \le f54 = f64 \le 5$
$\alpha 17 = 0.1$	$f91 = f121 = f141 = 0.5$
$\alpha 18 = 0.01$	$f92 = f122 = f142 = 1$
$0.001 \le \alpha 19 \le 100$	$0 \le f93 = f123 = f143 \le 5$
$\alpha 20 = 0.1$	$f101 = f131 = f151 = 1$
$\alpha 21 = 0.1$	$f171 = 1$
$0.001 \le \alpha 26 = \alpha 27 \le 100$	$f181 = 1$
	$f191 = 0.5$
	$f192 = 0.5$
	$f201 = 1$
	$f211 = 1$
	$f261 = f271 = 1$
	$0 \le f262 = f272 \le 5$

[a]Parameter estimates have been calculated using information from references.[13,15,16,18,22,36,39,63,74,77–82]

Parameter Values and Scanning Procedure

All 28 rate constants are positive. Because no inhibitory feedback is considered, all 52 kinetic orders are non-negative. The available data do not allow the determination of actual concentrations and absolute rates for many of the processes we need to consider. However, it does allow for the estimation of relative rates with respect to normal steady-state values of the different molecular species being considered. The same is true regarding the kinetic orders. Thus, by normalizing the equations with respect to standard steady-state values of the variable, we are able to study the qualitative behavior of the model. The basal values for rate constants and kinetic orders are given in Table AI.

The parameter scanning was done as follows: Kinetic orders have values that are bound by small integer numbers (between 0 and 5 in absolute value[66,74]). Because of the similarity between the two processes, it is reasonable to assume that the kinetic order of $AY1$ for the scaffold assembly of FeSC is the same in $v5$ and $v6$. Thus, we calculate the steady states of our model by keeping $f54 = f64$, and scanning for both between 0 and 5 at 0.5 intervals. Similarly, we keep $f93 = f123 = f143$ (influence of $AY1$ on the repair of FeSC) while we scan their values between 0 and 5 at 0.5 intervals. The final kinetic orders we scan measure the influence of $AY1$ on FeSC transfer from the scaffold proteins. Again, we consider that $f23 = f33 = f43 = f223 = f233$ while we scan their values between 0 and 5 at 0.5 intervals. Because our estimates of rates come from experiments done by different groups, under different conditions and sometimes using different systems, we also have sampled the ratio between different relative rates. We have sampled the ratio between the rate of de novo synthesis of FeSC and the rate of FeSC in situ repair, the rate of FeSC transfer to the cytoplasm and the ratio of Heme_Fe to FeSC synthesis, taking independent samples at different values for each of the ratios (0.001, 0.01, 0.1, 1, 10, 100). Additionally, we have repeated this experiment for the three different possible modes of FeSC transfer to apo-proteins (see Table III) and for the possibility that Arh1 does not act on FeSC through Yah1 ($\alpha 3 = \alpha 14 = \alpha 15 = \alpha 28 = 0$). Compounding this scanning with that for AY1 (0.001, 0.01, 0.1, 1, 10, 100), we calculated a total of approximately 7 million steady states, of which only the stable were used to compare with the experimental results.